# CHAPTER VII
## PREFERENTIAL CO OXIDATION OVER Au/ZnO-Fe$_2$O$_3$ IN AN INTEGRATED SYSTEM FOR H$_2$ FUEL PRODUCTION[*]

## 7.1 Abstract

In this research work, a fuel processing unit consisting of a methanol steam reforming (MSR) reactor over ShiftMax 240 (a commercial catalyst) and a preferential CO oxidation (PROX) reactor over the Au/ZnO-Fe$_2$O$_3$ catalyst was investigated. The MSR and PROX reactors were tested individually with the objective of optimizing operating conditions for minimum CO content. The results revealed that MSR gave a 100 % CH$_3$OH conversion at 250 °C. Moreover, the Au/ZnO-Fe$_2$O$_3$ catalyst prepared by photodeposition in the PROX reactor could remove the CO content in a H$_2$-rich stream to 0 ppm level, which is suitable for feeding to PEM fuel cells.

Keywords: Fuel processor system; Methanol steam reforming; Preferential CO oxidation; Photodeposition; Au catalyst; ZnO; Fe$_2$O$_3$

## 7.2 Introduction

At present, proton exchange membrane fuel cells (PEMFCs) are believed to be the candidate for vehicle applications or battery substitutions. Many of the advantages of PEMFCs are high efficiency, fast startup, low emissions of pollutants, and low noise [1,2]. Due to the lack of H$_2$ infrastructure technologies and the problem of H$_2$ storage, small scale H$_2$ production systems are required to find a practical process for supplying H$_2$, e.g. metal hydride (H$_2$ storage material) [3,4] and a hydrocarbon fuel processor [5,6,7]. Many types of fuel processors are being developed as potential H$_2$ suppliers to produce H$_2$ that is pure enough and that work fast enough to supply the PEMFCs. Among the hydrogen feeds, methanol is regarded

---

[*] In preparation.

as one of the most promising candidates for an onboard fuel processor. Many benefits of using methanol compared to ethanol are its high hydrogen/carbon ratio, moderate operating temperature, low coke formation, low sulfur compound content, and the fact that it can be produced from renewable resources [8]. In addition, the advantages of methanol steam reforming include the limited CO content and a higher $H_2$ content, compared to that of partial oxidation. The fuel processing system includes not only a $H_2$ production unit but also a CO removal unit because the products from a $H_2$ production unit always consist of $H_2$, $CO_2$, and CO. A small amount of CO in a $H_2$-rich stream can adsorb on the Pt anode catalyst in a PEMFC, causing the fuel cell performance to drop rapidly; therefore, it is necessary to remove the CO to less than 10 ppm (PEM fuel cell requirement) [9, 10]. There are many proposed processes to remove CO below the limit—pressure swing adsorption, membrane filtration, methanation [11,12,13], and the preferential oxidation of CO (PROX). PROX is considered to be a promising method in $H_2$ fuel [14]. Our research group has been studying the performance of prepared catalysts in a simulated reformate stream [15,16,17,18,19]. We found that Au-based catalysts exhibited high catalytic performance in terms of low temperature at maximum CO conversion, selectivity, and stability. For example, $Au/CeO_2$, prepared by co-precipitation, exhibited high activity at 110 °C. This preparation method created smaller Au particles (2 to 8 nm) that are active at lower temperatures. The $Au/FeO_x$ showed good stability and excellent activity in a $H_2$-rich stream under $CO_2$ and $H_2O$ at 50 °C. Recently, a $Au/ZnO-Fe_2O_3$ catalyst was prepared by photodeposition. This technique's advantages are: (1) a higher amount of Au is obtained; (2) heat treatment is not required since the gold is reduced by UV irradiation; and, (3) the Au particle size could be as small as ~1 to 2 nm [20]. Additionally, a PROX process has been developed by using a double-stage PROX reactor to enhance the process performance [18,21]. Our results clearly revealed that the double-stage PROX reactor greatly increases the CO selectivity, resulting in significant decrease in $H_2$ loss.

Hence, this article focuses on the development of an integrated fuel processing system consisting of a methanol steam reformer (MSR) and a double-stage PROX reactor. The methanol steam reforming tests were performed by using a

commercial Cu-based catalyst (Shiftmax 240), whereas the PROX tests were conducted on Au/ZnO-Fe$_2$O$_3$ with a 1% Au loading. Consequently, we have attempted to optimize the overall operating conditions in the methanol steam reformer in order to find the best outlet composition (the lowest CO content) that is suitable for direct feed into the PROX unit. In the PROX unit, the effects of reaction temperature on the catalytic performance and the catalytic stability were investigated. The composition of the effluent gas from the PROX unit is presented to show its ability to supply the PEMFCs.

## 7.3 Experimental

### 7.3.1 Catalyst preparation

A commercial CuO-ZnO catalyst, shiftmax 240 Süd-Chemie, was used as-received for MSR. For the PROX catalyst, ZnO-Fe$_2$O$_3$ was prepared by conventional co-precipitation between Zn(NO$_3$)$_2$.3H$_2$O (Sigma-Aldrich) and Fe(NO$_3$)$_3$.9H$_2$O (Fluka). The solution was kept at pH 8 with 0.1 M Na$_2$CO$_3$ (Riedel-de Haen), as described elsewhere [19]. To deposit nano-sized Au on the catalyst support, the photodeposition technique was employed. The starting concentration of HAuCl$_4$.xH$_2$O was controlled at 0.005 M to obtain 1 %atom Au; moreover, the power of the UV lamp and the contact time were fixed at 11 W and 3 h, respectively.

### 7.3.2 Catalytic activity measurement

The fuel processing was designed as a $H_2$ production process combined with a CO removal process, as shown in Figure 7.1.
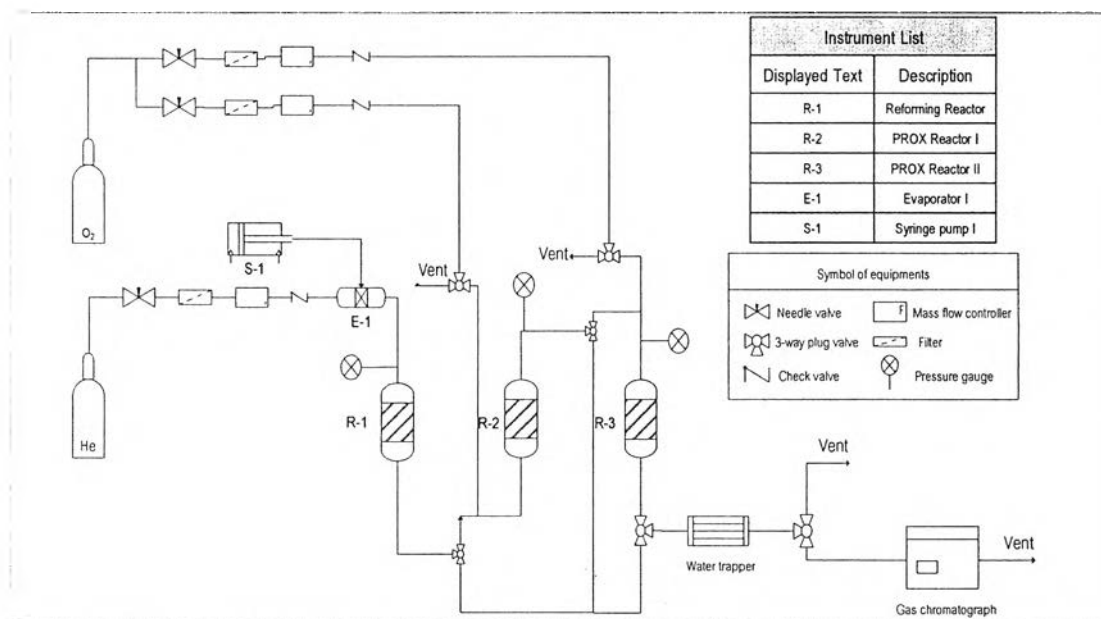


**Figure 7.1** Schematic of fuel processing system.

#### 7.3.2.1 MSR Unit

The MSR reaction was carried out in a fixed-bed reactor by packing with ShiftMax 240 under atmospheric pressure in the temperature range of 200 to 350 °C. A mixture of $CH_3OH$ (HPLC grade) and distilled water with a molar ratio of 1:1.3 was introduced by a syringe pump. Then, this mixture was vaporized in an evaporator. The mixture vapor was carried by He before entering the catalytic reactor and a He flow rate was maintained at 34 ml/min. The effluent gas was analyzed by an online gas chromatograph equipped with a packed carbosphere column (80/100 mesh and 10 ft x 1/8 inch) and a thermal conductivity detector (TCD), before entering the PROX unit. However, the condensate and byproduct were condensed in a condenser kept in an ice bath before analysis. The methanol conversion, $H_2$ selectivity, and $H_2$ yield were calculated by the following equations:

$$X = \frac{CO + CO_2 + CH_4}{MeOH_{(in)}} \cdot 100\% \qquad (7.1)$$

$$S_{H_2} = \frac{H_2}{H_2 + CH_4 + CO + CO_2} \cdot 100\% \tag{7.2}$$

$$Y_{H_2} = X * S_{H_2} \tag{7.3}$$

Where

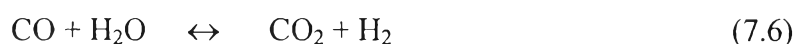| | |
|---|---|
| X | = methanol conversion (%) |
| MeOH$_{(in)}$ | = mole of methanol inlet |
| S$_{H2}$ | = hydrogen selectivity (%) |
| Y$_{H2}$ | = H$_2$ yield (%) |
| H$_2$ | = amount of hydrogen in the product stream |
| CO | = amount of carbon monoxide in the product stream |
| CO$_2$ | = amount of carbon dioxide in the product stream |
| CH$_4$ | = amount of methane in the product stream |

### 7.3.2.2 PROX Unit

The residual CO in the reformed gas was removed by oxidation with $O_2$ over the Au/ZnO-Fe$_2$O$_3$. The double-stage reactor was employed for PROX under realistic conditions (CO, CO$_2$, H$_2$, and H$_2$O composition) from the MSR unit. The amount of O$_2$ feeding was controlled at $\lambda$=2. O$_2$ was individually added to the reformed gas in each PROX reactor with a split ratio of 50:50, and it had a temperature controller to achieve the desired temperature. The temperature was varied between 30 and 110 °C. The total amount of catalyst (Au/ZnO-Fe$_2$O$_3$) was calculated based on the total feed flow rate from the MSR unit with a space velocity of the total gas mixture (GHSV) of 30,000 h$^{-1}$, and the catalyst packed equally in each reactor. The outlet products from the first reactor were sent directly to the second reactor. The product was monitored by an online gas chromatograph. No catalyst pretreatment process was used prior to the activity tests. The process performance was presented in terms of CO conversion, selectivity, and CO content in the products. The CO and O$_2$ conversions were calculated based on the consumption of CO and O$_2$, respectively. The selectivity towards CO oxidation was defined as the

ratio of $O_2$ consumption for the desired CO oxidation reaction to the total $O_2$ consumption. All measurements were conducted until steady state was reached.

## 7.4 Results and Discussion

### 7.4.1 MSR Performance

Pepply et al. [22] proposed that there are many pathways for the production of $H_2$ and $CO_2$ by MSR. The MSR reaction (7.4) takes place together with methanol decomposition (7.5) and water-gas shift reactions (7.6).

$$CH_3OH + H_2O \quad \leftrightarrow \quad 3H_2 + CO_2 \qquad (7.4)$$

$$CH_3OH \quad \leftrightarrow \quad CO + 2H_2 \qquad (7.5)$$

$$CO + H_2O \quad \leftrightarrow \quad CO_2 + H_2 \qquad (7.6)$$

*7.4.1.1 Effect of Reaction Temperature*

From the above reactions (7.4–7.6), minor CO content comes from the methanol decomposition reaction. As exothermic reactions, the CO content increases with increasing temperature but a higher methanol conversion can also be achieved at high temperatures in order to produce more $H_2$ fuel. Therefore, the operating temperature should be optimized for the maximum $H_2$ production with minimum CO content. Figure 7.2 shows the MSR process performance at a contact time (W/F) of $2.93 \times 10^{-3}$ $g_{cat}{}^*min/ml$ as a function of reaction temperature. The result revealed that both $CH_3OH$ conversion and $H_2$ yield have a similar trend, which increases with increasing the reaction temperature, because both reforming and decomposition of methanol reactions are very endothermic reactions. In a temperature range of 250 to 350 °C, these values slowly reduce; however, CO content noticeably rises from 950 ppm at 200 °C to nearly 3 % vol 350 °C when the contact time was $2.93 \times 10^{-3}$ $g_{cat}{}^*min/ml$. The $H_2$ selectivity is independent on the reaction temperature. Moreover, the highest $CH_3OH$ conversion over ShiftMax 240 was achieved at 250 °C, which

provided 87 % $CH_3OH$ conversion, 75 % $H_2$ selectivity, and 65 % $H_2$ yield. At this temperature, a CO content of around 0.7 %vol was produced, which is suitable to feed directly to the PROX unit without passing through further auxiliary units.
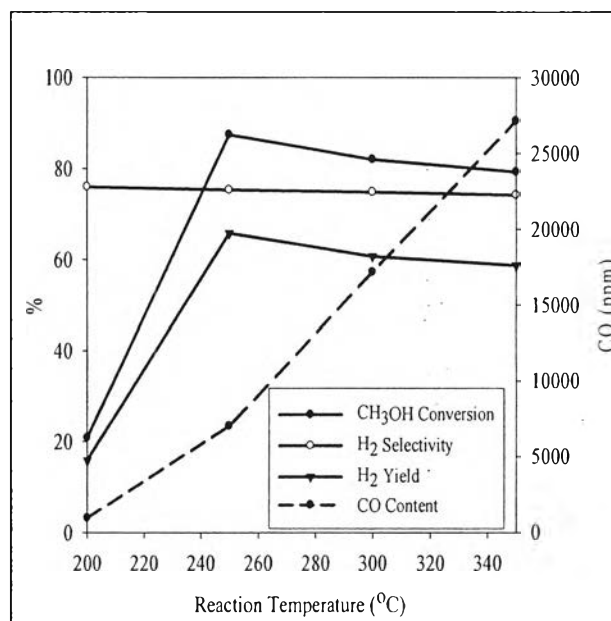


**Figure 7.2** The performance of the MSR process over the ShiftMax 240 catalyst at W/F = 2.93 × 10⁻³ $g_{cat}$*min/ml.

Additionally, another possibility for CO formation would be a reverse water-gas shift (RWGS) reaction. The RWGS reaction is endothermic; therefore, the high temperature (230 to 300 °C) will facilitate the formation of CO, which does not depend on the catalyst support or the synthesis method [23]. Moreover, the RWGS reaction easily takes place in the presence of $CO_2$ in the reformate. Based on the above criteria, a temperature of 250 °C was selected as the optimum temperature for operating MSR over ShiftMax 240. Nevertheless, the stability of the catalyst in the MSR process is emphasized for operating the system. Figure 7.3 shows a stability test of the MSR reaction over ShiftMax 240 with W/F = 2.93 × 10⁻³ $g_{cat}$*min/ml at 250 °C. The result clearly reveals that the process provided a fluctuating performance; however, its overall performance was still high. Additionally, CO

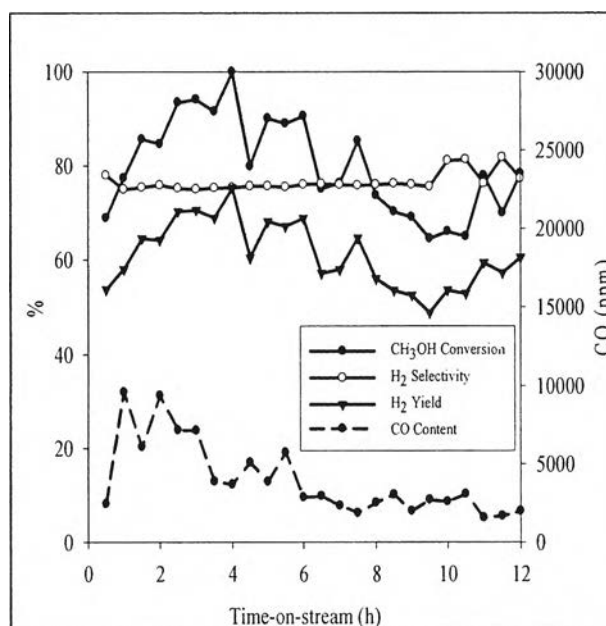content remained below 1 % vol, and $H_2$ selectivity was not influenced in the period of 1 to 9 h.



**Figure 7.3** Stability testing of the MSR reaction over ShiftMax 240 with W/F = 2.93 $\times\ 10^{-3}$ $g_{cat}$*min/ml at 250 °C.

*7.4.1.2 Effect of Contact Time*

The MSR reaction was performed at a contact time variation in the range of 2.9 $\times$ $10^{-3}$ to 2.9 $\times$ $10^{-2}$ $g_{cat}$*min/ml, shown in Figure 7.4. The effect of contact time on $CH_3OH$ conversion and $H_2$ yield at 250 °C is clearly seen as they were enhanced with increasing contact time; however, it did not affect $H_2$ selectivity (Figure 7.4a). At low contact time (2.9 $\times$ $10^{-3}$ to 5.8 $\times$ $10^{-3}$ $g_{cat}$*min/ml), $CH_3OH$ conversion and $H_2$ yield remarkable increased from 87 % to 96 % and 66 % to 83 %, respectively. At longer contact time, a higher conversion is attained (100 % $CH_3OH$ conversion).
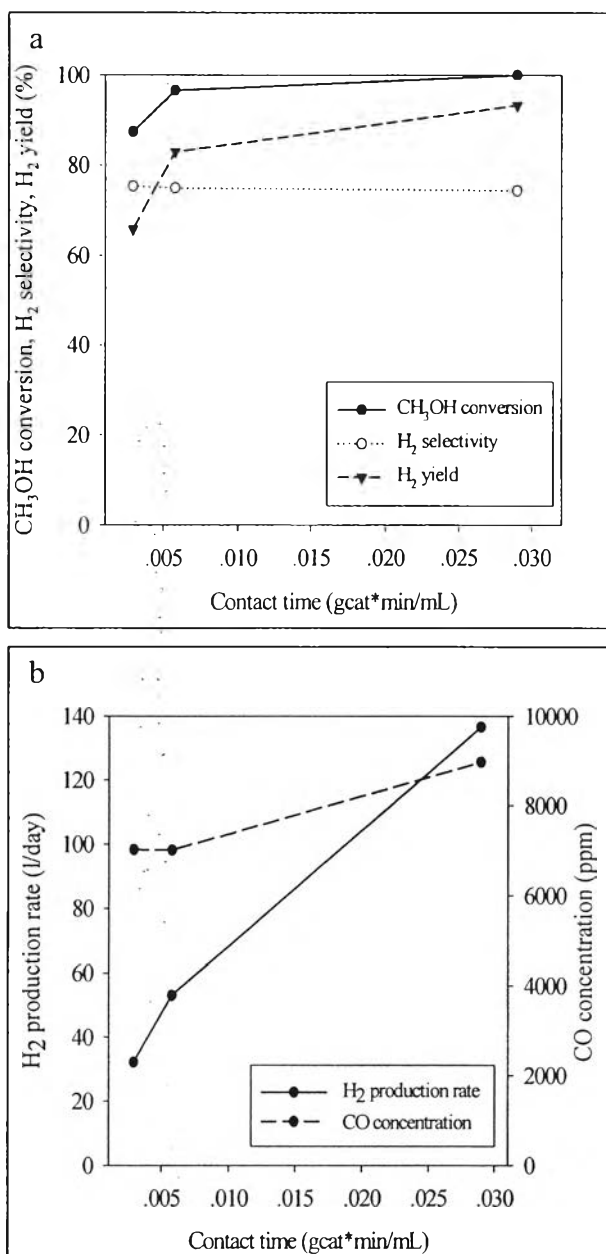
**Figure 7.4** Effect of contact time on the MSR process performance over ShiftMax 240 at 250 °C: (a) $CH_3OH$ conversion (-●-), $H_2$ selectivity (·○·), and $H_2$ yield (-▼-); (b) $H_2$ production rate (-●-) and CO content (-●-).

Similarly, $H_2$ production rate and CO content in methanol reformate increase with increasing the contact time, as shown in Figure 7.4b. At these conditions, the MSR provided the highest $H_2$ production rate at 136.6 l/day. However, the CO content in the reformate gas is less than 1 %vol in all experiments, suggesting that the $H_2$-rich stream from the MSR could be sent directly to the PROX

without further CO removal. Based on those results, a contact time of $2.9 \times 10^{-2}$ $g_{cat}^{*}$min/ml was selected as the best condition for producing a high amount of $H_2$ fuel with an acceptable level of CO. Furthermore, another advantage of this condition is the absence of $CH_3OH$ in real reformate because 100 % $CH_3OH$ conversion was reached. This implies that we can reduce the influence of $CH_3OH$ in the PROX catalytic activity. Since $CH_3OH$ acts as an inhibitor of CO oxidation, as reported by Avgouropoulos et al. [24].

The ShiftMax 240 exhibited high activity, and the catalyst life was also evaluated under $CH_3OH$ and water with a molar ratio of 1:1.3. Figure 7.5 shows the product distribution from the gas phase of the MSR over ShiftMax 240 at 250 °C at a contact time of $2.9 \times 10^{-2}$ $g_{cat}^{*}$min/ml. The result reveals that $H_2$ and $CO_2$ are main components in the methanol reformate, combined with a small amount of CO. Another product ($CH_4$) was not observed in this process. Additionally, this process exhibited a stable catalytic process under monitoring time.
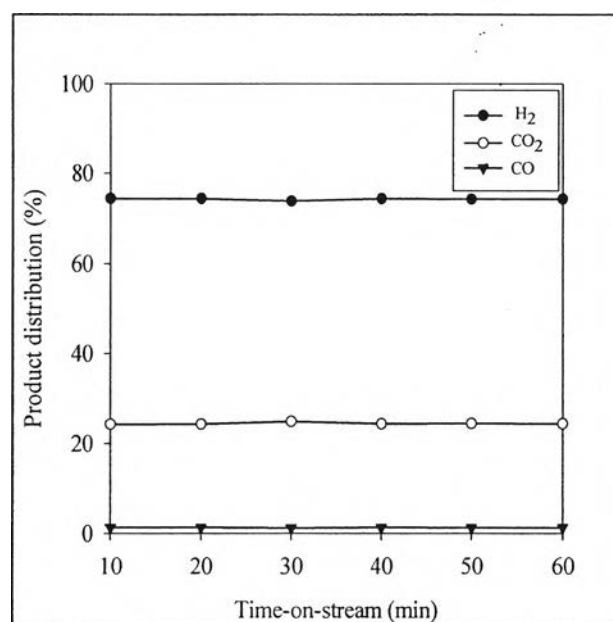


Figure 7.5 Product distribution of the MSR over ShiftMax 240 at 250 °C with contact time of $2.9 \times 10^{-2}$ $g_{cat}^{*}$min/ml.

### 7.4.2 PROX Performance

As mentioned before, PROX is frequently used for the purification of reformate due to the limited CO tolerance of the Pt anode of a PEMFC. Thus, the CO conversion in reformed gas and the effect of reaction temperature on catalytic performance is discussed.

#### 7.4.2.1 Single-Stage Reactor

To examine the possibility of prepared catalyst that can be utilized under realistic conditions from the MSR unit. The single-stage PROX reactor was employed. In this work, the PROX was carried out over a $Au/ZnO-Fe_2O_3$ catalyst prepared by a photodeposition. The oxidation of residual CO by adding $O_2$ reduces the CO content in the reformate to below 10 ppm. Our observation indicates that the catalyst has a high potential for operating under realistic conditions with MSR (Figure 7.6). Complete CO conversion (100%) was obtained at 30 °C and slightly dropped to 90 % at 70 °C with further raising the reaction temperature, CO conversion decreased to around 40 % at 130 °C. In terms of selectivity, at 30 °C, the catalyst gave a maximum selectivity of 58 % and then also followed a similar trend as CO conversion in that the selectivity decreased with a raising of the reaction temperature. On the other hand, the catalytic process consumed $O_2$ and rapidly reached 100% at 50 °C. These results agree well with the studies of similar catalysts from our group [25], which revealed that the $Au/ZnO-Fe_2O_3$ catalyst is very active and selective at low temperatures (30–50 °C). The decrease in selectivity with increasing temperature was attributed to competitive $H_2$ oxidation at higher reaction temperature.
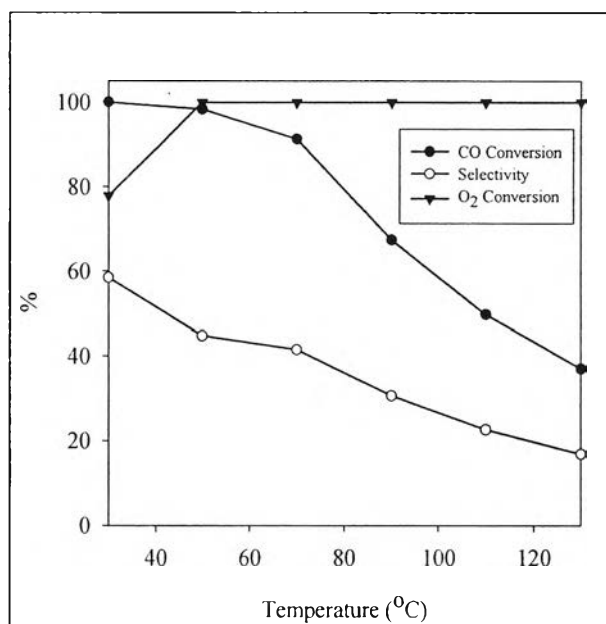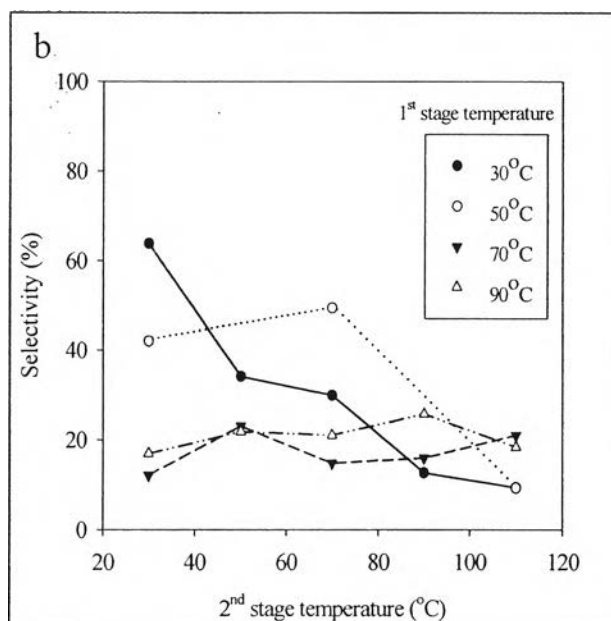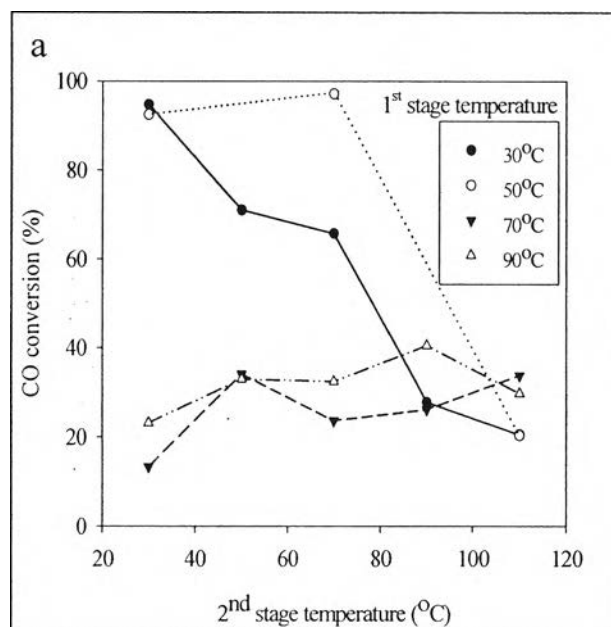
**Figure 7.6** Effect of reaction temperature on the catalytic activities of Au/ZnO-Fe$_2$O$_3$ in a single-stage PROX reactor under realistic conditions from the MSR unit: CO conversion (●), selectivity (○), and O$_2$ conversion (▼).

*7.4.2.2 Double-Stage Reactor*

A double-stage PROX process was utilized for the CO removal process because the amount of O$_2$ added to reactor can be reduced by optimizing the addition of O$_2$ in each stage. The double-stage experiment was performed under the same reaction conditions as the single-stage process, except for the fractionation of an amount of O$_2$. Nevertheless, the double-stage PROX performance depends on many parameters, such as the temperature at each stage, the O$_2$ split ratio, and so on. Our previous results showed that the O$_2$ split ratio has little effect on the process performance but the operating temperature at each stage has a significant influence [21]. For the optimization of the operating conditions for a double-stage reactor in the PROX unit in order to achieve the best performance, the temperature in each stage is an important factor. In these experiments, the O$_2$ split ratio was constant at 50:50 and the effect of reaction temperature on the process performance was observed. The PROX unit was tested between 30 and 110 °C. These experiments were performed under real reformed gas from MSR unit. All products (H$_2$, CO$_2$, and

CO) from the MSR unit were sent directly to the double-stage PROX unit, and then the final product was analyzed by an online gas chromatograph to indentify the PROX process. Figure 7.7a shows the effect of reaction temperature in each stage on the CO conversion of $Au/ZnO-Fe_2O_3$. This observation is in accordance with previous work. The catalyst is very active at low temperatures, which provided almost 100 % CO conversion. Further raising the reaction temperature in the 1st and/or 2nd stages led to a reduction of the CO conversion. It is clear that the catalytic activity fluctuated greatly, resulting from the fact that the MSR process performance is not constant, as described above. When comparing the CO conversion of the double-stage to the single-stage process, the maximum CO conversion of the double-stage process is slightly less than that of the single-stage process. This phenomenon might be explained by the effect of $CO_2$ on the catalytic performance of $Au/ZnO-Fe_2O_3$. $CO_2$ was generated from both the MSR and the CO oxidation reactions. Previously, we studied this effect in simulated reformate, and the results indicated that the addition of $CO_2$ would lead to a severe reduction in the catalytic activities, resulting in decreased CO conversion. In addition, the CO conversion was more influenced by the first stage temperature at higher temperatures (70 to 90 °C). However, at low temperatures, CO conversion was not greatly impacted. This occurrence may be explained in that the process cannot achieve a desired temperature at the second stage or cannot reduce the reaction temperature from the first stage to the desired temperature at the second stage as we would like, resulting in severe CO conversion decreases at high temperatures. Similarly, the selectivity of $Au/ZnO-Fe_2O_3$ in the double-stage showed the same trend as the CO conversion. Figure 7.7b shows the effect of reaction temperature in each stage on the selectivity of $Au/ZnO-Fe_2O_3$. The maximum selectivity of the prepared catalyst was usually obtained at low temperature range. Nevertheless, the process cannot reduce the second stage temperature to the desired temperature if the temperature in the first stage is too high. Figure 7.7c compares the measured $O_2$ conversion for two sets of reaction temperatures in each stage. The results showed that $O_2$ conversion is generally higher with increasing the second stage temperature but the first stage temperature did not have much influence. Based on the observation, the suitable operating temperature in the double-stage PROX process has to be operated in the

same or near temperature at a low temperature range. The first- and second-stage temperature at 30 °C is a selected condition for operating the PROX unit over the Au/ZnO-Fe$_2$O$_3$ catalyst.
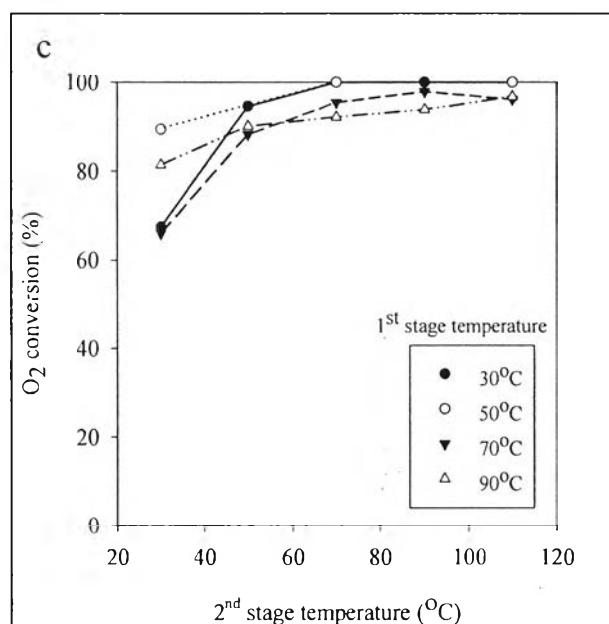
**Figure 7.7** Effect of reaction temperature on the catalytic activities of $Au/ZnO-Fe_2O_3$ in a double-stage PROX. The temperature of the first stage was controlled at 30 °C (●), 50 °C (○), 70 °C (▼), and 90 °C (▽). The temperature of the second stage was varied in the temperature range of 30 to 110 °C: (a) CO conversion, (b) selectivity, and (c) $O_2$ conversion.

Since the fuel processor will be applied to a PEMFC for vehicle applications, the stability of process is a vital factor. Figure 7.8 illustrates the stability of the fuel processor, which is a combination of MSR and PROX units. These experiments revealed that the process performance exhibited good stability under the operating conditions within the monitored reaction period and then started deactivating after 3 h. A slight decay was observed until 4 h; after that, the process performance was improved by flushing the accumulated $H_2O$ with He at 110 °C for 30 min. Then, a high process performance was observed again. However, the catalytic activity and stability of both MSR and PROX catalysts should be developed to provide better fuel processing performance.
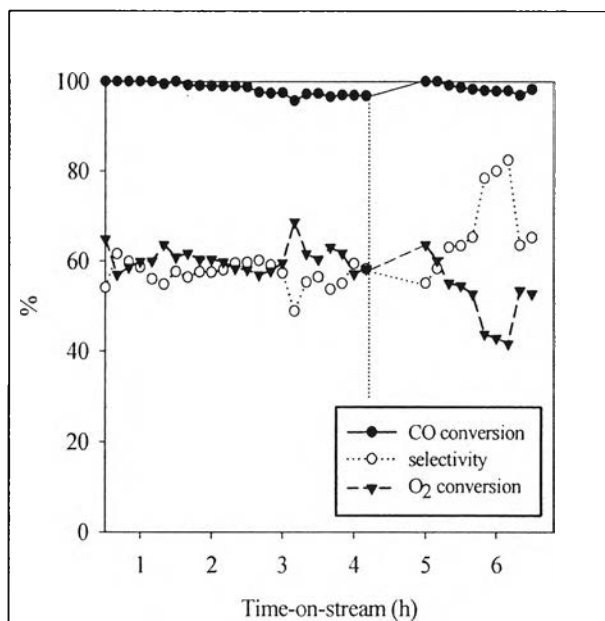
Figure 7.8 Stability testing of Au/ZnO-Fe₂O₃ in a double-stage PROX at 30 °C: CO conversion (●), selectivity (○), and O₂ conversion (▼).

## 7.5 Conclusions

A small fuel processor, consisting of MSR and PROX reactors, was studied; and the effects of the main operating parameters on CO conversion were also studied. The MSR operated at 250 °C, which provided the highest $CH_3OH$ conversion (100 %) over ShiftMax 240, combined with 75 % $H_2$ selectivity, and 65 % $H_2$ yield. At a high process performance of the MSR, the CO content from the MSR was lower than 1 vol%. The results showed that the reactor performance depends on the reaction temperature and contact time. Additionally, Au/ZnO-Fe₂O₃ prepared by a photodeposition can be utilized in a PROX unit under realistic conditions from the MSR unit, and complete CO conversion can be achieved, in order to remove the CO content to 0 ppm before feeding the pure $H_2$ fuel to the PEMFC.

## 7.6 Acknowledgement

## 7.7 References

[1]     V. Mehta, J.S. Coope, Review and analysis of PEM fuel cell design and manufacturing, J. Power Sources 114(1) (2003) 32–53.

[2]     A. Heinzel, B. Vogel, P. Hübner, Reforming of natural gas—hydrogen generation for small scale stationary fuel cell systems, J. Power Sources 105 (2002) 202–207.

[3]     J.D. Kim, Y.I. Park, K. Kobayashi, M. Nagai, Effect of CO gas and anode-metal loading on $H_2$ oxidation in proton exchange membrane fuel cell, J. Power Sources 103 (2001) 127–133.

[4]     W.M. Yan, H.S. Chu, M.X. Lu, F.B. Weng, G.B. Jung, C.Y. Lee, Degradation of proton exchange membrane fuel cells due to CO and $CO_2$ poisoning, J. Power Sources 188 (2009) 141–147.

[5]     D.J. Moon, J.W. Ryu, K.S. Yoo, D.J. Sung, S.D. Lee, Development of iso-octane fuel processor system for fuel cell applications, Catal. Today 136 (2008) 222–227.

[6]     A. Cutillo, S. Specchia, M. Antonini, G. Saracco, V. Specchia, Diesel fuel processor for PEM fuel cells: Two possible alternatives (ATR versus SR), J. Power Sources 154 (2006) 379–385.

[7]     Y. Chen, H. Xu, Y. Wang, X. Jin, G. Xiong, Hydrogen production from liquid hydrocarbon fuels for PEMFC application, Fuel Process. Technol. 87 (2006) 971–978.

[8]     M. Manzoli, A. Chiorino, F. Boccuzzi, Decomposition and combined reforming of methanol to hydrogen: a FTIR and QMS study on Cu and Au catalysts supported on ZnO and $TiO_2$, Appl. Catal. B-Environ. 57 (2005) 201–209.

[9] J.D. Kim, Y.I. Park, K. Kobayashi, M. Nagai, Effect of CO gas and anode-metal loading on $H_2$ oxidation in proton exchange membrane fuel cell, J. Power Sources 103 (2001) 127–133.

[10] W.M. Yan, H.S. Chu, M.X. Lu, F.B. Weng, G.B. Jung, C.Y. Lee, Degradation of proton exchange membrane fuel cells due to CO and $CO_2$ poisoning, J. Power Sources 188 (2009) 141–147.

[11] S.E. Iyuke, W.R.W. Daud, A.B. Mohamad, A.A.H. Kadhum, Z. Fisal, A.M. Shariff, Application of Sn-activated carbon in pressure swing adsorption for purification of $H_2$, Chem. Eng. Science 55 (2000) 4745–4755.

[12] Y. Chen, Xu H, Wang Y, Jin X, Xiong G. Hydrogen production from liquid hydrocarbon fuels for PEMFC application. Fuel Process Technol 2006;87:971–978.

[13] Choudhury MBI, Ahmed S, Shalabi MA, Inui T. Preferential methanation of CO in a syngas involving $CO_2$ at lower temperature range. Appl Catal A-Gen 2006;314:47–53.

[14] Choudhary TV, Goodman DW. CO-free fuel processing for fuel cell applications. Catal Today 2002;77:65–78.

[15] Luengnaruemitchai A, Osuwan S, Gulari E. Selective catalytic oxidation of CO in the presence of $H_2$ over gold catalyst. Int J Hydrogen Energy 2004;29:429–435.

[16] Luengnaruemitchai A, Thoa DTK, Osuwan S, Gulari E. A comparative study of $Au/MnO_x$ and $Au/FeO_x$ catalysts for the catalytic oxidation of CO in hydrogen rich stream. Int J Hydrogen Energy 2005;30:981–987.

[17] Naknam P, Luengnaruemitchai A, Wongkasemjit S, Osuwan S. Preferential catalytic oxidation of carbon monoxide in presence of hydrogen over bimetallic AuPt supported on zeolite catalysts. J Power Sources 2007;165:353–358.

[18] Luengnaruemitchai A, Nimsuk M, Naknam P, Wongkasemjit S, Osuwan S. A comparative study of synthesized and commercial A-type zeolite-supported Pt catalysts for selective CO oxidation in $H_2$-rich stream. Int J Hydrogen Energy 2008;33:206–213.

[19] Naknam P, Luengnaruemitchai A, Wongkasemjit S. Au/ZnO and Au/ZnO-Fe$_2$O$_3$ prepared by deposition–precipitation and their activity in the preferential oxidation of CO. Energ Fuel 2009;23(10):5084–5091.

[20] Chang LH, Yeh YL, Chen YW. Preferential oxidation of CO in hydrogen stream over nano-gold catalysts prepared by photodeposition method. Int J Hydrogen Energy 2008;33:1965–1974.

[21] Naknam P, Luengnaruemitchai A, Wongkasemjit S. Investigation of double-stage preferential CO oxidation reactor over bimetallic Au–Pt supported on A-zeolite catalyst. Ind Eng Chem Res 2008;47:8160–8165.

[22] Peppley BA, Amphlett JC, Kearns LM, Mann RF. Methanol–steam reforming on Cu/ZnO/Al$_2$O$_3$. Part 1: the reaction network. Appl Catal A-Gen 1999;179:21–29.

[23] Purnama H, Ressler T, Jentoft RE, Soerijanto H, Schlögl R, Schomäcker R. CO formation/selectivity for steam reforming of methanol with a commercial CuO/ZnO/Al$_2$O$_3$ catalyst. Appl Catal A-Gen 2004;259:83–94.

[24] Avgouropoulos G, Papavasiliou J, Ioannides T. PROX reaction over CuO-CeO$_2$ catalyst with reformate gas containing methanol. Catal Commun 2008;9:1656–1660.

[25] Naknam P, Luengnaruemitchai A, Wongkasemjit S. Preferential CO oxidation over Au/ZnO and Au/ZnO-Fe$_2$O$_3$ catalysts prepared by photodeposition. Int J Hydrogen Energy 2009;34:9838–9846.